Proceedings of the 9th Biennial ASME Conference on Engineering Systems Design and Analysis
ESDA08
July 7-9, 2008, Haifa, Israel

ESDA2008-59473

HIGH STIFFNESS CLOSED-FORM KINEMATIC STRUCTURAL DESIGN OF A LOW-COST 4/5-AXIS MICRO/MESO-SCALE INVERTED HIGH-SPEED MACHINING CENTER

Prof. J.Rhett Mayor
Asst. Professor

Mr. Edward Kimn
Undergraduate Research Assistant

Precision Manufacturing Research Center
The George W. Woodruff School of Mechanical Engineering
Georgia Institute of Technology
Atlanta, Georgia, 30332, USA

ABSTRACT

The demand for miniaturized components is increasing in various industries, such as the biomedical, consumer electronics, optics and defense-related industries. The production of the micro/meso-scale components and parts in these industries is typically undertaken using MEMS-type photolithographic production techniques that have limitations in the materials and geometries that can be produced. However, numerous research efforts during the course of the last five to ten years have developed micro-scale EDM processes, micro-laser processes and micro-machining operations. In particular, the micro-machining processes have been demonstrated to provide a credible solution to the production of micro/meso-scale parts with complexes geometries in a broad range of materials. The development of mMTs is growing with the rapidly increasing demand for tighter tolerances. Traditionally, mMTs have been developed based on horizontal or vertical Cartesian co-ordinate machine tool structures. However, as the need for increased process flexibility and productivity is continuously being driven higher, there is a need to develop higher degree of freedom machining systems, including 4-axis and 5-axis machining centers. In this paper, the design of a low-cost, high-precision, high-speed 4/5-axis micro/meso machining center is presented as a cost-competitive alternative to existing open-form kinematics precision machining centers. A key departure from traditional machine tool design approach that has been adopted in this design is the utilization of closed-form kinematic structural design to create a high-stiffness, low-cost machine tool base. In addition, the lower thermal mass of the mMT base enhances rapid thermal washout in the structure and significantly reduces the thermal gradients in the structure. Consequently the thermal errors present in the structure are limited and simply and adequately handled using existing error compensation strategies. Initial results from an analytical and numerical investigation of the thermo-mechanical response of an innovative, kinematically closed-form inverted micro-machining center are presented. A coarse resolution parametric study was undertaken to evaluate the preferred preferred design space for maximum stiffness and minimum thermal distortion in low-cost, high precision, high-speed micro-machining centers. In addition, in order to facilitate part loading and unloading operations will be considered as a key design characteristic. A key result of this study has been the identification of a preferred design space for kinematic form selection, material selection and structural design options for increased rigidity, reduced thermal error and reduced production costs for flexible 4/5-axis micro/meso-scale machining centers. The proposed mMT design achieves a 3X increase in rigidity over a comparable tradition kinematically open horizontal mMT system

1. INTRODUCTION

The demand for miniaturized components is increasing in various industries, such as the biomedical, consumer electronics, optics and defense-related industries. The production of the micro/meso-scale components and parts in these industries is typically undertaken using MEMS-type photolithographic production techniques that have limitations in the materials and geometries that can be produced. However, numerous research efforts during the course of the last five to ten years have developed micro-scale EDM processes, micro-laser processes and micro-machining operations. In particular, the micro-machining processes have been demonstrated to provide a credible solution to the production of micro/meso-scale parts with complexe geometries in a broad range of materials. The development of mMTs is growing with the rapidly increasing demand for tighter tolerances. While the pace of development of mMT technology has accelerated during the recent past, the remaining limiting factors for micro-mechanical machining are the miniaturization of the components, tools, and processes [1].

Originally, the process of meso-scale machining relied on 3-axis motion. Vogler et al. used a 3-axis micromachining tool that allowed for 25x20x25 mm movement in the x, y, and z-axes, respectively, that relied on 1 μm resolution linear encoders for positioning feedback [2]. For the tool, they used a 150,000 rpm, air-turbine spindle with a 3.175 mm diameter chuck. Another 3-axis motion machine was used by Lee et al. with an overall machine size of 300x150x150 mm in a horizontal working position. The linear stages were driven by a PZT actuator working on an inchworm mechanism which resulted in a 100 nm resolution. The air-turbine spindle operated at a maximum speed of 120,000 rpm with a milling tool diameter of 0.2 mm [3]. Lee et al. [4] also used a 3-axis machine that used piezoelectric stages to move 50x50x14 mm in the x, y, and z-axes, respectively. The air turbine spindle had a highest speed of 145,000 rpm and a spindle runout of 1 μm.

With the development of more intricate parts, the mMTs require more versatility. In order to grant more flexibility to cut different angles of the part, researchers have begun working with 5-axis cutting machines. Bang et al. [5] designed a 5-axis milling machine with three precision linear stages and two precision rotary stages. The linear stages have a 20x20x30 mm travel range in the x, y, and z-axes, respectively, and a 50 nm resolution. The rotary stages have a 360o range of motion. The a-axis* stage, which holds the workpiece, has a resolution of 0.0012o, while the spindle on the c-axis* stage has a resolution of 0.002o. The air motor spindle was used with a range of speed of 20,000-30,000 rpm [5]. As an example of machining a complicated geometrical part, Takeuchi et al. [6] designed an ultraprecision 5-axis milling machine to produce a hig-precision, high surface quality micro components, and demonstrated the capabilities of the machine by producing a micro-scale replication of a Buddha's head. Their system consisted of an air-born linear guide and air-slider for the x and z-axes, respectively. The y-axis table had a 20 mm stroke and the table could rotate in the a-axis. The resolution of the tables and rotation axes were 1 nm and 0.000001^{o}. They also used an air-turbine spindle for milling with a speed of 55,000 rpm [7]. A prototype 5-axis mMT, developed at the University of Illinois at Urbana-Champaign was used by Phillip et al. [7]. The machine had approximately 0.3 m2 of a footprint. The linear stages used rolling element bearings which provided 40 mm of travel in the x, y, and z-axes. The a-axis had 360o of travel using the rotary stage and the c-axis had 180o of motion with another rotary stage, both of which used air bearings. The brushless AC linear motors had a 20nm resolution with optical linear encoders while the rotary motors had 0.316 arcsec resolution optical rotary encoders.

The current mMT's have been developed based on traditional horizontal or vertical Cartesian co-ordinate machine tool structures. The goal of this research is to investigate the thermo-mechanical response of an innovative, inverted-spindle mMT structure and dvelop a preferred design space for maximum stiffness and minimum thermal distortion. In addition, means to facilitate part loading and unloading operations will be considered as a key design characteristic. The fourth axis will be the c-axis which will allow the spindle to rotate to create more rigid tool to workpiece contact. The purpose of using an inverted milling machine is to help with chip removal which will reduce the risk of damaging the tool or causing imperfections in the workpiece. This paper will review the design of the 4-axis machine based on material selection, rigidity, and the kinematic description based on the layout.

2. DESIGN CONCEPT GENERATION FOR 4-AXIS INVERTED MICRO-MACHINING CENTER

The design objectives for the 4-axis micro-machining center were to a) achieve high structural rigidity through closed kinematics design, b) achieve a minimum mass, minimum cost design, c) achieve a minimum resolution (encoder, or basic length unit (BLU) of 0.050μm for the linear stages and 0.001 radians for the rotational axis, d) facilitate rapid load/unload operations and ease of interface to material handling systems and e) pursue a inverted spindle design to take advantage of improved chip evacuation for high-speed machining operations. The basic kinematic strucutre considered was a two-axis XY stacked stage to form the machining surface on the part-to-ground leg, and a separate, inverted Z-axis stacked on the rotational stage attached to the base plane forming the tool-to-ground leg. Several design concepts were generated with the primary variations being in the mechanisms considered for the rotational fourth axis. Goniometer-based design variants were considered and rejected due to mass penalties of the drives, overall bulkiness of the implementation and a negative impact on the structural rigidity of the machine tool frame caused by the need for large clearance heights on the Z-column. Further consideration was given to the use of universal rotator actuators which were discarded again due to the high stage mass and the negative impact of the mass on the Z-stage dynamics.

The final design concept for the four-axis inverted meso-scale machining tool is presented in Figure 1. The design concept follows the desired kinematics, achieving a closed form strucutre that supports the primary machining surface in an inverted position above the spindle sub-structure. The spindle structure is cantilevered off the cloased frame, illustrated on the left side in Figure 1 The design concept has been built around existing stage technology, implementing Aerotech ANT-50L stages for the XY-linear stages, capable of achieving 0.005μm encoder resolution, and max speed and acceleration of 250mm/s and 2.5g respectively. The spindle movement is provided by motorized crossed roller bearing linear stage for the z-axis and a rotary stage for the c-axis. A brushless motor and spindle is used to provide the high cutting speeds.

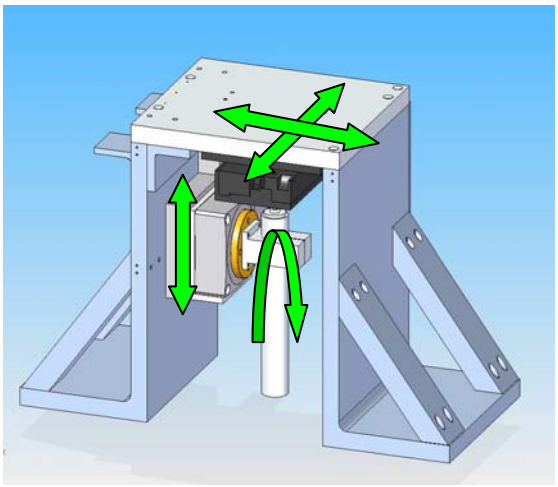

Figure 1. A solid model of the initial design concept for the 4-axis inverted meso-scale machining center. The axis motions are illustrated with green arrows.

The overall size of the machine workspace is 202 mm x 220 mm x 203 mm (W x D x H) with an additional 100 mm for clearance for the spindle. the plate used to mount the xy-stage was later modified to the current hinged plate that could be opened in order to have easier access to the stages and spindle. When closing the top, the plate is located by guides and locator pins and held down by screws. The supporting walls are made from structural angle and the side support plates are removable to allow easier from the sides.

3. FEA DESIGN ENHANCEMENTS FOR IMPROVED STRUCTURAL RIGIDITY

The natural frequencies of the system were necessary for analysis on the structural rigidity of the system and a redesign. To determine whether the system would be rigid, it was compared to a study previous done by Lee et al. [**Error! Bookmark not defined.**], a scaled conventional milling machine was created where the harmonic frequencies were found using an FEA program. The results from that study are presented in **Error! Reference source not found.**, and have been used as the baseline for minimum acceptable receptances in the structure. In order to complete the modal analysis, the spindle was removed from the system in order to test the integrity of the structure and not the whole system. Another modification to the FEA model was a simplification of the solid models of the stages due to their complex geometry. The linear ANT stages and rotary stage were created by approximately recreating their geometries and forcing a density for the properties to simulate the real model. The FEA model created in ALGOR multi-physics for the original design is shown in Figure 2.

Table 1. Natural frequencies found from previous study of conventional micromachine [4]

	Natural Frequencies (Hz)	
Modes	Cast iron	Aluminum
1st	248.5	361.3
2nd	271.1	394.2
3rd	644.5	937.2
4th	778.2	1131.6

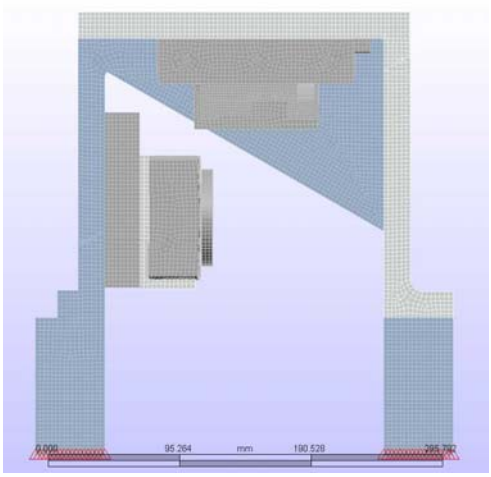

Figure 2. FEA Model used to evaluate the structural rigidity of the 4-axis mMT design concept.

The natural frequency of the first mode was calculated to be 370 Hz. Because the natural frequency of the conventional machine was found to be approximately 250-360 Hz, an alternative design was considered to improve the stiffness of the mMT frame. Analysis of the displaced model results from the modal analysis clearly demonstrated that the initial deformation mode was in the x-direction, with the mass of the XY-stages creating a bending mode of the structure in that direction, shown in Figure 3. As a result, the new model design based on the previous analysis, shown in Figure 1, was transferred to ALGOR to complete a modal analysis. The analysis was completed on a design consisting of mainly aluminum plates, then steel, and then a hybrid. The purpose of testing different materials was because while steel is a much stiffer material over aluminum, because the machine is inverted, most of the weight is at the top of the machine. The result is that the weight at the top acts as an inverted pendulum and is thus much more unstable. With aluminum, the density is much lower meaning less mass will be at the top of the structure. The redesigned model and the mesh used on that structure is shown in Figure 4.

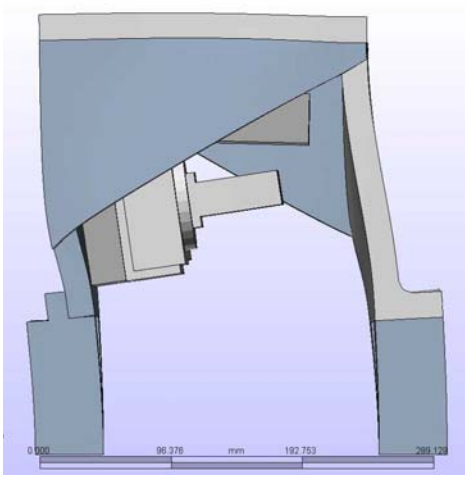

Figure 4. Displaced model results from FEA of the original design concept showing instability of the frame in the x-direction.

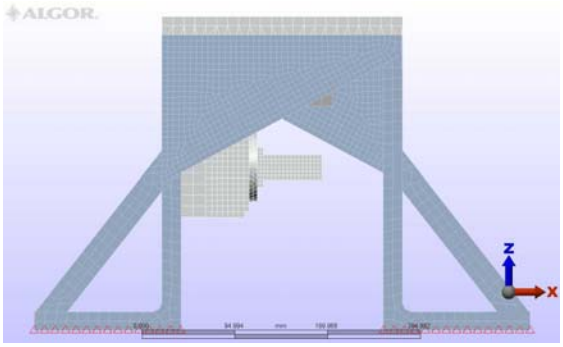

Figure 5. Redesigned model with mesh

The analysis of structure resulted in a significant increase in the harmonic frequency. It reduced the first mode movement into the x-direction as shown in Figure 8 which is the hybrid model where the back plate, also referred to as the tombstone, where the z-linear stage and rotary stage are mounted, is made of AISI 1020 cold rolled steel and the top and front plate is made of aluminum 6061 T-6. A summary of the harmonic frequencies with the different materials is shown in Table 2.

Table 2. Summary of modal analysis

	Original Design	Redesign		
Modes	Steel	Aluminum	Steel	Hybrid
1st	369.4	709.6	668.2	763.3
2nd	776.2	771.9	838.8	799.6
3rd	899.9	874.4	922.8	891.2
4th	1209.3	993.4	1021.0	1046.1

From the table the redesigned model has a much higher natural frequency by a factor of 3.07 for the previous study and 2.07 over the original inverted design. Since the hybrid had the highest first natural frequency over the considered redesigns, it was the chosen model based on harmonic frequencies.

4. THERMO-MECHANICAL DESIGN EVALUATION

The thermal expansion of the structure can have significant impact on the operational accuracy achievable with the system, and therefore the design was analyzed to ensure minimum thermal gradients under expected themal loading for various material selections. Aluminum tends to spread the heat through the whole volume much quicker than steel and so for the case of this machine where there are power losses and released heat from cutting, the temperature distribution is important to determine deformations. In order to find the steady-state thermal distribution, the boundary conditions were estimated. For the study completed, it was assumed that ambient temperature would be at 25°C and nodal temperatures started at 25°C. The system was assumed to only undergo free convection; specifically, the effects of buoyancy. From Incropera and DeWitt [8] the equations for free convection were found for the conditions that would apply to the machine. Only 4 cases applied to the system: vertical plates, inclined plates, upper surface heated plates/lower surface cooled plates, and lower surface heated plates/upper surface cooled plates. Table 3 lists the varibales used in the steady state thermal study, particularly for the calculation of the free convection boundary conditions applied in the FEA steady state thermal model.

Table 1. Variables used for free convection calculations

Nomenclature	
Ra_L	Rayleigh's number
g	Gravity constant
β	Volumetric thermal expansion coefficient
T_s	Surface temperature
T_∞	Ambient temperature
L	Characteristic length
υ	Kinematic viscosity of fluid
α	Thermal diffusivity
Pr	Prandtl's number
$\overline{Nu}_L$	Nusselt's number
k	Thermal conductivity
$\bar{h}$	Convection coefficient

For each case, the Rayleigh's number, Ra_L, was calculated using

$$Ra_L = \frac{g\beta(T_S - T_\infty)L^3}{\upsilon\alpha} \quad (1)$$

For the case of the inclined plate, gravity is defined as,

$$g = g\cos\theta \quad (2)$$

where θ is the angle between the vertical and the incline plane. For the case of the horizontal plates, L is defined as,

$$L = \frac{A_S}{P} \quad (3)$$

where A_s is the surface area and P is the perimeter. In the case of the vertical or inclined plates, L is just the length along the plate in the vertical direction. The volumetric thermal expansion coefficient, β, was just the inverse of the temperature of interest. All other fluid properties were found through linear interpolation of data given by Incropera and DeWitt [8] at the film temperature. Once Rayleigh's number was found the Nusselt's number was found, where Nu_L is defined as,

$$\overline{Nu}_L = 0.68 + \frac{0.670 Ra_L^{1/6}}{[1+(0.492/Pr)^{9/16}]^{4/9}} \quad (4)$$

$$\overline{Nu}_L = 0.54 Ra_L^{1/4} \quad (5)$$

$$\overline{Nu}_L = 0.27 Ra_L^{1/4} \quad (6)$$

where (9) was used for vertical and inclined plates, (10) was used for upper surface heated plates/lower surface cooled plates, and (11) was used for lower surface heated plates/upper surface cooled plates. All structural surfaces were treated either as cooled surfaces, while the stages surfaces were treated as heated surfaces. After Nusselt's number was found, the convective coefficient was found by,

$$\bar{h} = \frac{\overline{Nu}_L k}{L} \quad (7)$$

The calculated convection coefficient was calculated for a range of temperatures for each surface subject to free convection. The coefficients and corresponding temperatures were imported into ALGOR to determine a load curve for each individual open surface. The program automatically calculated the necessary convective coefficient as it was finding the steady-state temperatures. The stages and spindle were all considered heat generators. It was assumed that they had an 80% efficiency, meaning that it loss 20% of its power to heat. It was also assumed that all stages and the spindle produced the same power of 300W. Therefore, the power lost was 60W and the heat generation was the power loss divided by the volume of each stage or spindle.

Applying the convection conditions to the applicable surfaces and the heat generations to the stages and spindle, the steady-state analysis was conducted and the minimum temperature was found to be 60.7°C while the maximum temperature was found to be 133.6°C. The temperature distribution can be seen in Figure .

Given the thermal output from the previous analysis, a static stress analysis was conducted. This analysis determined where the maximum stresses and displacements would be located due to the thermal expansion and under the effects of gravity. The maximum displacement occurs at the front edge of the top plate with a maximum of 0.649 mm, as shown in Figure 7.

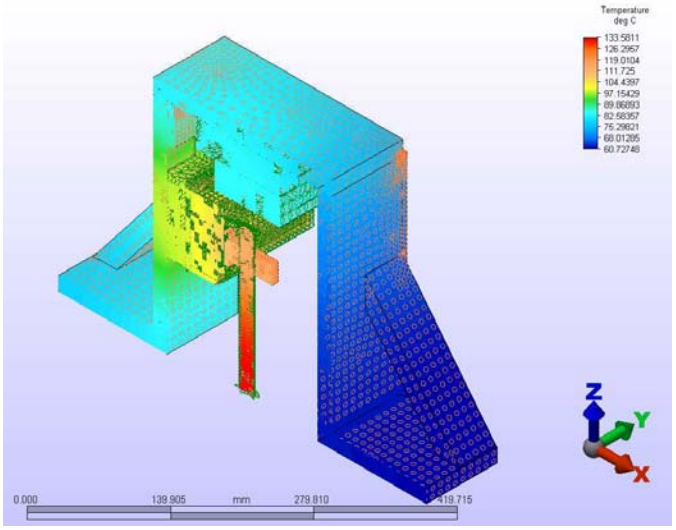

Figure 6. Temperature distribution throughout the system

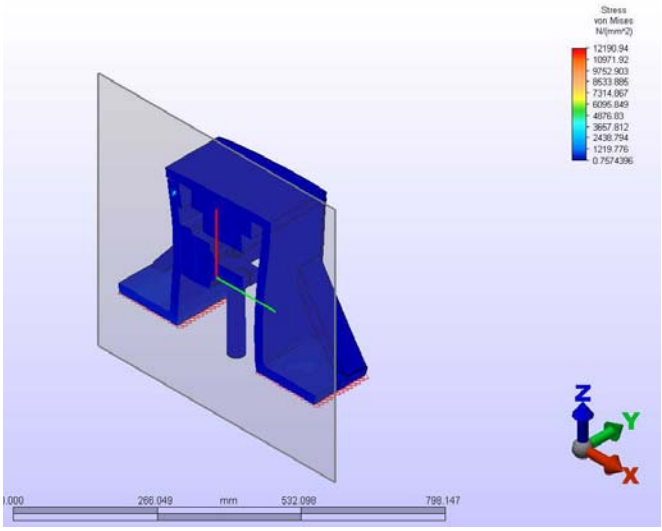

Figure 7. Results from the thermo-mechanical FEA analysis indicate maximum thermal distortion of the frame to be 650μm.

5. DISCUSSION

The harmonic analysis of the original structure showed that it was rigid compared to the previous study performed by Lee et al. However, to increase the safety factor, the structure was made given more support to help reduce the first mode. The change increased the natural frequency by almost a factor of two. The next part of the modal analysis was material selection and the effects on the harmonic frequencies. Based on the analysis of the two extreme cases of all steel and all aluminum, the hybrid selected had the highest natural frequency. Even

though steel is more rigid than aluminum, the steel is also denser than the aluminum. Therefore, if the top plate was made from steel, the more mass would be concentrated at the top which would help increase the effects on the mode shape.

From Figure 9, the hottest temperature occurs in the spindle as expected. The spindle has a lower density so the heat generated throughout that small volume would produce the most heat. The temperatures may be higher than reality because it was estimated that all the stages would produce 300W of power with a power loss of 60W. However, in actuality, the stages may produce less power than that or may be more efficient. Another consideration is the stages were producing 300W of power, but they may not be producing that power constantly since the stages will not be in a constant state of motion.

The maximum stress from the thermal load was extremely high. However this is believed to be an exaggerated stress due to the type of contact selected by ALGOR. Between the top plate and the angled support, the program is seeing a bonded contact which means the nodes are fixed together and not allowed to separate without stiffening. However, in the real case, they would be allowed to separate and only stiffen if forced against each other. More variations in the lower stress color spectrum would be visible if it were not for the high stress which changes the scale. The stresses from the thermal load are not expected to be very high because the stress is directly proportional to the strain. Since the material is not expected to expand very much, which is part of strain, the stress should not be that higher either.

While the results from FEA are informative, they are not completely accurate results. The FEA model had simplifications for geometry purposes. The holes were removed from the structure because the interaction between the parts was the point of study for this paper. Another introduction of deviation was the assumption of power for the thermal analysis. The power generated by the stages and spindle might not be as high as estimated for the FEA model so the temperatures, stresses, and displacements could potentially be lower than the model represents. The FEA model gives an approximation of the structure's capability, but at a high estimate.

6. CONCLUSIONS

The chosen design was 3 linear stages, 1 rotary stage, and a high-speed air spindle in an inverted setup, which aims to help with chip removal from the part. Meso-scale milling machines have proven to be more precise than full sized conventional machines because of their capabilities with tolerances. The system passes the criteria of being structurally reliable according to the modal analysis in ALGOR with a 1st mode natural frequency at 763.3 Hz, while being able to withstand major thermal expansions and stresses. A hybrid of material selection was chosen in order to maintain the structural integrity and withstand thermal expansions. Through analysis, it was determined that a combination of steel and aluminum would be used. The tombstone was made from steel because of the weight and moments acting on the wall. Aluminum was chosen for the top and front plates because of their light weight, stiffness, and thermal diffusivity. Being an inverted milling machine, the next objective would be to observe how the chip removal and cutting operation compares to a conventional method.

7. REFERENCES

[1] Chae, J., Park, S.S., and Freiheit, T., 2006, "Investigation of Micro-cutting Operations," International Journal of Machine Tools and Manufacture, **46**(3), pp. 313-332.

[2] Vogler, M.P., DeVor, R.E., and Kapoor, S.G., 2004, "On the Modeling and Analysis of Machining Performance in Micro-endmilling, Part i: Surface Generation," Journal of Manufacturing Science and Engineering, Transactions of the ASME, **126**(4), pp. 685-694.

[3] Lee, J.H., Park, S.R., and Yang, S.H., 2006, "Machining a Micro/meso Scale Structure Using a Miniaturized Machine Tool by Using a Conventional Cutting Process," Journal of Manufacturing Science and Engineering, **128**(3), pp. 820-825.

[4] Lee, S.W., Mayor, R., and Ni, J., 2006, "Dynamic Analysis of a Mesoscale Machine Tool," Journal of Manufacturing Science and Engineering, **128**(1), pp. 194-203.

[5] Bang, Y.B., Lee, K.M., and Oh, S., 2005, "5-Axis Micro Milling Machine for Machining Micro Parts," International Journal of Advanced Manufacturing Technology, **25**(9), pp. 888-894.

[6] Takeuchi, Y., Yonekura, H., and Sawada, K., 2003, "Creation of 3-D Tiny Statue by 5-Axis Control Ultraprecision Machining," CAD Computer Aided Design, **35**(4), pp. 403-409.

[7] Phillip, A.G., Kapoor, S.G., and DeVor, R.E., 2006, "A New Acceleration-based Methodology for Micro/meso-scale Machine Tool Performance Evaluation," International Journal of Machine tools and Manufacture, **46**(12), pp. 1435-44.

[8] Incropera, F.P. and DeWitt, D.P., 2002, *Fundamentals of Heat and Mass Transfer*, 5th ed., John Wiley & Sons, Inc. New Jersey, pp. 545 – 552, 917.

[9] Norton, R.L., 2006, *Machine Design: An Integrated Approach*, 3rd ed., Pearson Prentice Hall. New Jersey, pp. 282, 944, 948

[10] Gere, J.M., 2001, *Mechanics of Materials*, 5th ed., Brooks/Cole, California, pp. 94.